Molecular Tensile Testing Machines: Breaking a Specific Covalent Bond by Adsorption-Induced Tension in Brushlike Macromolecules

Insun Park and Sergei S. Sheiko*

Department of Chemistry, University of North Carolina at Chapel Hill, Chapel Hill, North Carolina 27599-3290

Alper Nese and Krzysztof Matyjaszewski

Department of Chemistry, Carnegie Mellon University, 4400 Fifth Avenue, Pittsburgh, Pennsylvania 15213

Received December 2, 2008
Revised Manuscript Received February 6, 2009

Recently, we have reported that covalent bonds may spontaneously break upon adsorption of brushlike macromolecules onto a substrate.[1,2] The intramolecular tension is self-generated due to steric repulsion between densely grafted side chains. Adsorption enhances the chain crowding and results in amplification of bond tension from the piconewton to nanonewton range.[3] We have also shown that this tension is evenly distributed throughout the central part of the brush backbone, leading to random scission of its carbon−carbon (C−C) bonds, while the scission probability decreases at the ends of the backbone.[1,3] Here we address a challenging problem: how to break only one specific bond within a macromolecule, leaving other bonds intact. In order to endow tension with the single-bond selectivity, we designed a brushlike macromolecule with a disulfide (S−S) bond in the middle of the all-carbon polymethacrylate backbone (Figure 1). Since the disulfide bond is weaker than the surrounding C−C, C−O, and C−S bonds, one expects its predominant scission. To verify this hypothesis, we performed a series of control experiments on a model polymer which contains a linker with one monosulfide bond and two ester bonds. Brushlike molecular architecture with a weak linker in the midsection of the backbone can be regarded as a miniature tensile testing machine, wherein the brush part generates tension and transmits it to the linker, enabling single-bond studies of mechanically activated chemical reactions. One of the distinctive features of the developed molecular tool is that the force is generated spontaneously without using external fields and single molecule devices. This takes forward the current efforts in molecular mechanochemistry.[4−13]

Atom transfer radical polymerization (ATRP)[14,15] was used to prepare two kinds of brush polymers with a disulfide bond and a monosulfide bond in the middle of the backbone. Both polymers have two ester groups in the linker. The polymers consist of a poly(2-hydroxyethyl methacrylate) backbone and poly(*n*-butyl acrylate) side chains. We have prepared two disulfide-containing polymers with the number-average degree of polymerization (DP) of the backbone $2N = 1300$ and DP of the side chains $n = 60$ and 130, respectively (Supporting Information 1, Scheme S1). In the case of the polymer with the monosulfide linker, DP of the backbone is $2N = 1000$ and DP of the side chains is $n = 120$ (Supporting Information 1, Scheme S2). Brush molecules were deposited onto the surface of water/2-propanol mixtures in Langmuir−Blodgett (LB) trough from a dilute solution in chloroform. The surface energy of the liquid substrate was fine-tuned by changing the concentration of 2-propanol and controlling its vapor pressure.[2] After different exposure times (time spent on the air/water interface), monolayers were transferred to a mica substrate for imaging individual molecules by atomic force microscopy (AFM).

Figure 2 demonstrates AFM images and length distributions of brush molecules with longer side chains ($n = 130$) on four different liquid substrates. The length distributions were obtained from two 3×3 μm AFM images, including about 720 molecules to ensure a relative standard deviation of the mean below 4%. Clearly, molecules undergo fracture which depends on the surface energy. On the substrate with the lowest surface energy (Figure 2a), one observes the characteristic bimodal distribution with two main peaks at ∼160 and ∼320 nm. This distribution represents the original as-synthesized sample. To verify this claim, we have studied brushes with shorter side chains ($n = 60$) resulting in a lower tension (<1 nN), which is insufficient for breaking covalent bonds within reasonable period of time (days).[2,16] In Supporting Information 2, we show that the length distribution of short-side-chain brushes does not change with time and does not depend on the substrate type (Figure S3). The initial bimodality of brush length could result from the disulfide cleavage during esterification and also from the partial reduction of the disulfide bond, which is sensitive to radical transfer reactions. The disulfide cleavage could be additionally accelerated by the electron transfer process from ATRP catalyst.

The intrinsic bimodality is very favorable for this study as it provides a clear reference for the midchain cleavage. When the surface tension was raised, the molecular fraction at $L \cong 320$ nm decreased, while the fraction of shorter molecules at $L/2 \cong 160$ nm correspondingly increased (Figure 2b,c). The midchain fracture is due to preferential scission of the disulfide linker, which occurs at a much faster rate compared to the stronger C−C bonds in the same backbone (Figure 1). The C−C scission becomes noticeable upon raising the surface energy of the liquid substrate (Figure 2c,d). The fracture of the C−C backbone is a random process which leads to broadening of the first peak due to the emergence of molecules shorter than 160 nm.

To quantitatively compare the scission rate of the S−S bond with the surrounding C−C, C−O, and C−S bonds (Figure 1), we studied the scission kinetics of brushes with an all-C backbone and brushes with a monosulfide linker (Supporting Information 1, Scheme S2). Figure 3a shows representative AFM images of brush molecules with S−S and C−S linkers along with the corresponding temporal variations of the number-average contour length (Supporting Information 3, Table S5). Molecular imaging allows two complementary methods for the analysis of the kinetics of bond scission. The first method is based on measuring the number-average contour length (L_n) which decreases upon scission. The second method is based on monitoring the number of molecules (Γ) per unit area which increases upon scission. Both methods are complementary since the product of Γ and L_n gives the total number of covalent bonds per unit area. From these two methods, we prefer the length analysis which is more accurate as it does not depend on

* To whom correspondence should be addressed. E-mail: sergei@email.unc.edu.

10.1021/ma8026996 CCC: $40.75
Published on Web 03/02/2009

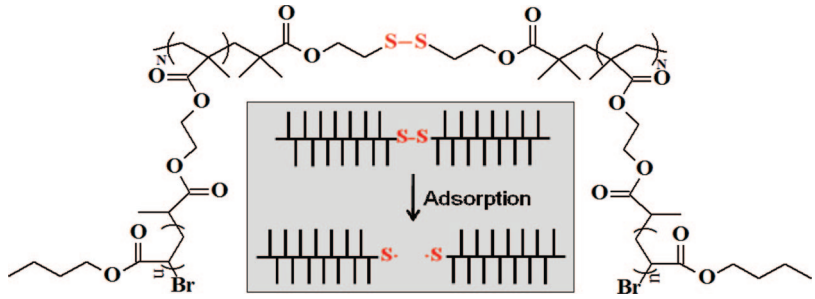

Figure 1. Chemical structure of brushlike macromolecule ($N = 650$ and $n = 60$ or 130) having a single disulfide bond in the middle of the backbones. Scheme (inset) shows the midchain fracture of the backbone due to the adsorption-induced tension.

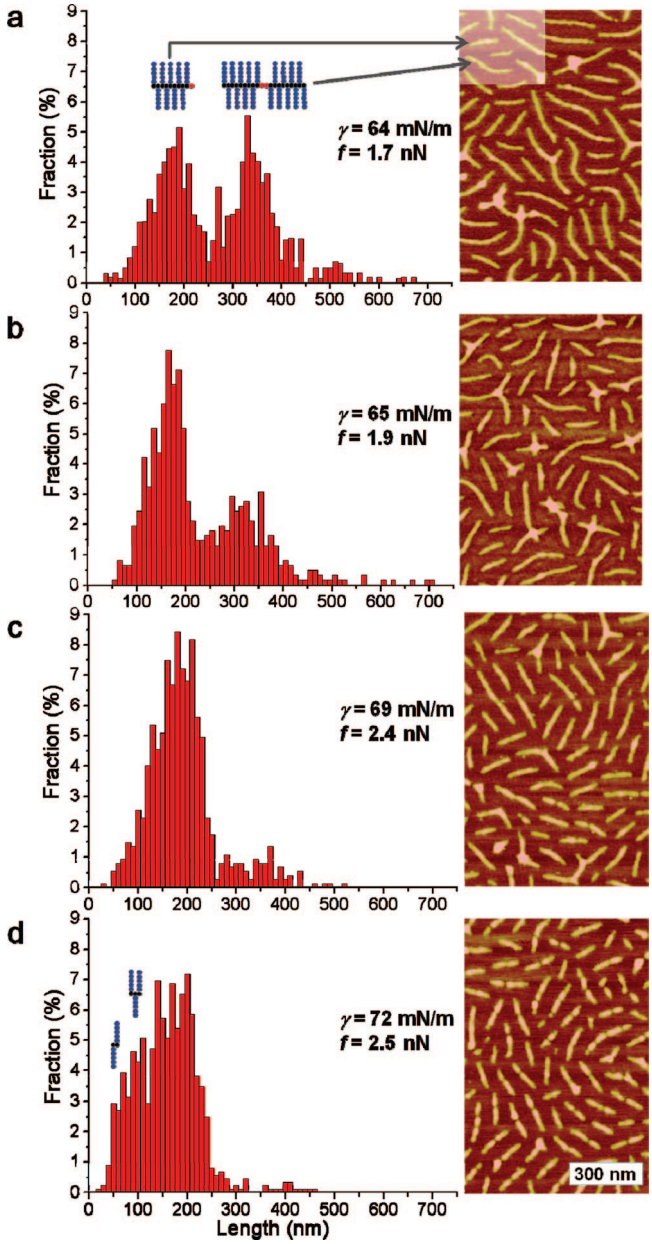

Figure 2. AFM height images along with the corresponding length distributions were measured for brush molecules with long side chains ($n = 130$) transferred to a mica substrate. Prior to transfer, the molecules were deposited for 30 min onto four liquid substrates with different surface tensions (γ) determined by the concentration of 2-propanol: (a) 1.0%, (b) 0.9%, (c) 0.3%, and (d) 0% (pure water). The highlighted area of the AFM image in (a) demonstrates the original and midchain fractured molecules that lead to the bimodal length distribution. For each system, the tension was calculated as $f = S \times d$, where $d = n \times 0.25$ nm is the brush width, n is the DP of the side chains, and $S = \gamma_s - \gamma_l - \gamma_{sl}$ is the spreading parameter, defined as difference between the surface free energies of substrate−gas (γ_s), liquid−gas (γ_l), and substrate−liquid interfaces (γ_{sl}).

variations of surface coverage (number molecules per unit area) due to sample preparation. In order to obtain the time dependence of the contour length L, we assume that bond scission is a first-order reaction described by the equation

$$\Phi = \frac{A}{A_0} = e^{-kt} \tag{1}$$

where $A = \Gamma(m - 1)$ is the number of bonds per unit area, Γ is the number of molecules per unit area, and $m = \Gamma(L_n/L_\infty - 1)$ is the effective degree of polymerization, where L_∞ is the contour length of polymer chains at infinite time, i.e., the length of an effective monomer. By assuming that every bond scission results in a new molecule ($\partial A/\partial t = -\partial\Gamma/\partial t$), one obtains the following time dependence for the contour length:

$$\left(\frac{1}{L} - \frac{1}{L_\infty}\right) \Big/ \left(\frac{1}{L_0} - \frac{1}{L_\infty}\right) = e^{-kt} \tag{2}$$

where L_0 is the contour length at $t = 0$. For the disulfide-containing brushes, one can use $L_0 = 2L_\infty$ since the molecules effectively contain two monomers of length L_∞.

Equation 2 was used to fit the experimental data points using the rate constant k as a single fitting parameter. Figure 3b shows the corresponding fitting curves along with the measured L_0 and L_∞ values in the figure caption. The following rate constants have been obtained: $k = 4.3 \times 10^{-4}$ s^{-1} for brushes with the S−S linker, $k = 7.5 \times 10^{-6}$ s^{-1} for brushes with the C−S linker, and $k = 1.5 \times 10^{-6}$ s^{-1} and $k = 9.6 \times 10^{-8}$ s^{-1} for all-carbon brushes with $n = 110$ and $n = 80$, respectively. The significant difference in rate constants between S−S and C−S linker strongly suggests that midchain scission of S−S containing linkers occurs due to scission of the S−S bonds rather than the surrounding C−C, C−S, and C−O bonds (Figure 1). It is also evident that the C−C scission is significantly slower compared to both C−S and S−S bonds. Under the nearly same force S−S bond breaks at a lifetime of $\tau = 1/k = 2.3 \times 10^3$ s while C−C bond remains nearly intact due to the significantly longer lifetime, $\sim 10^7$ s. The significantly lower stability of disulfide bonds is consistent with its relatively low dissociation energy ($E_{S-S} = 268$ kJ/mol, $E_{C-S} = 255$ kJ/mol, $E_{C-C} = 347$ kJ/mol, and $E_{C-O} = 351$ kJ/mol) and the significantly longer bond length ($l_{S-S} = 2.03$ Å $> l_{C-S} = 1.82$ Å $> l_{C-C} = 1.54$ Å $> l_{C-O} = 1.43$ Å).[17]

In addition to the analysis of the number-average length, the rate constant can be directly obtained by monitoring the number of long (prior-to-scission) molecules. This approach is accurate for midchain scission, resulting in a bimodal distribution with clearly separated distribution bands (Figure 2). Note that the number fraction of the disulfide linkers (eq 1) exactly corresponds to the number fraction of the prior-to-scission molecules, which was obtained from the length distribution histograms by integrating the area of the distribution band at $L \cong 320$ nm ranging from 265 to 715 nm (see arrow in

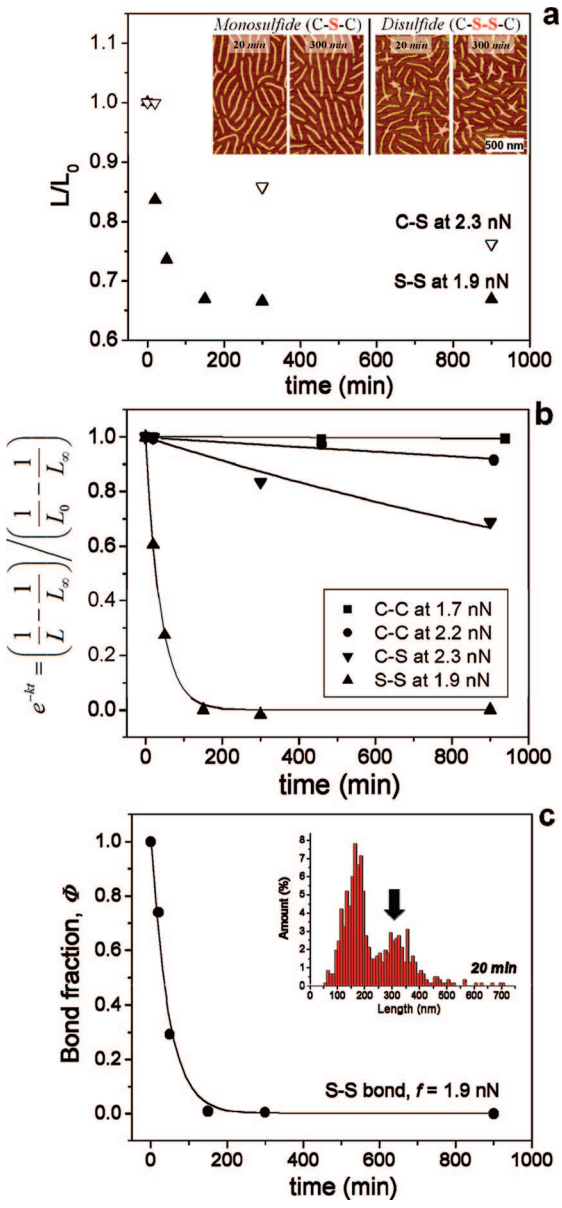

Figure 3. Contour length of brushlike macromolecules with different midchain linkers has been monitored as a function of time spent on a surface of water/propanol mixtures. Their behavior is compared to brushes with all-carbon backbones, i.e., without linkers. (a) Number-average contour length of brushes with the S−S and C−S midchain linkers decreases with time. The disulfide-containing brushes demonstrate significantly faster decay even at a lower tension of 1.9 nN. Inset: AFM height micrographs of brushes with disulfide and monosulfide linkers captured at shorter and longer times. (b) The fraction of covalent bonds ($\Phi = A/A_0 = e^{-kt}$) was obtained from the analysis of the number-average contour length for all-C−C brushes as well as brushes with C−S and S−S bonds in the middle of the backbone. The solid lines correspond to eq 2 using the following measured values for L_0 and L_∞: for S−S, $L_0 = 269$ nm and $L_\infty = 180$ nm (assuming midchain scission); for C−S, $L_0 = 290$ nm and $L_\infty = 145$ nm (assuming midchain scission); for C−C, $L_0 = 750$ nm and $L_\infty = 65$ nm (assuming random scission). (c) Number fraction of disulfide linkers (concentration of reactants) as a function of time was obtained by integrating the area of the length distribution band at $L \cong 320$ nm ranging from 265 to 715 nm (see arrow). The bond tension (see numbers in nN) is calculated as $f \cong S \times d$ where S is the spreading parameter, $d = n \times 0.25$ nm is the brush width, and n is the DP of side chains. For the disulfide containing brushes ($n = 130$) and a surface of a 99.1/0.9 wt % water propanol mixture ($S = 17.5$ mN/m), the adsorption generates a bond tension of 1.9 nN. On the same substrate, the two all-C−C brushes ($n = 80$ and 110) develop a tension of 1.7 and 2.2 nN, respectively. Brushes with a monosulfide bond undergo tension of 2.3 nN on pure water ($S = 22.5$ mN/m).

the inset in Figure 3c). Figure 3c shows the data points along with the fitting curve from eq 1. This method gives a rate constant of 3.7×10^{-4} s^{-1}, which is similar to $k = 4.3 \times 10^{-4}$ s^{-1} obtained from the length analysis.

To summarize, we have designed brushlike macromolecules that are able to focus tension to a single disulfide bond leading to its scission while other bonds remain intact. As such, these molecules can be used as a miniature tool for mechanical activation of chemical reactions at specific chemical bonds. The applied force can be finely tuned in a broad range from 10 pN to 10 nN by varying either the substrate surface energy or the brush structure (grafting density, side chain length, and degree of branching).[3] For very dense brushes, the tension linearly increases with the degree of polymerization of the side chains as $f \cong S \times N$, where S is the spreading parameter.[1−3] Accurate control of tensile forces in the piconewton−nanonewton range allows applications of the developed molecular tool to a wide range of covalent and noncovalent bonds. We also imagine that the new tool will be used in combination with other activation stimuli, such as temperature, electric field, and light.

Acknowledgment. We gratefully acknowledge funding from the National Science Foundation (DMR 0606086, CBET-0609087) and Petroleum Research Fund (46204-AC7).

Supporting Information Available: Polymer synthesis and characterization. This material is available free of charge via the Internet at http://pubs.acs.org.

References and Notes

(1) Sheiko, S. S.; Sun, F. C.; Randall, A.; Shirvanyants, D.; Rubinstein, M.; Lee, H.-i.; Matyjaszewski, K. *Nature (London)* **2006**, *440*, 191–194.
(2) Lebedeva, N. V.; Sun, F. C.; Lee, H.-i.; Matyjaszewski, K.; Sheiko, S. S. *J. Am. Chem. Soc.* **2008**, *130*, 4228–4229.
(3) Panyukov, S. V.; Zhulina, E. B.; Sheiko, S. S.; Randall, G.; Brock, J.; Rubinstein, M. *J. Phys. Chem. B* **2008**, in press.
(4) Bhasin, N.; Carl, P.; Harper, S.; Feng, G.; Lu, H.; Speicher, D. W.; Discher, D. E. *J. Biol. Chem.* **2004**, *279*, 45865–45874.
(5) Carl, P.; Kwok, C. H.; Manderson, G.; Speicher, D. W.; Discher, D. E. *Proc. Natl. Acad. Sci. U.S.A.* **2001**, *98*, 1565–1570.
(6) Sandal, M.; Grandi, F.; Samori, B. *Polymer* **2006**, *47*, 2571–2579.
(7) Ainavarapu, S. R. K.; Wiita, A. P.; Dougan, L.; Uggerud, E.; Fernandez, J. M. *J. Am. Chem. Soc.* **2008**, *130*, 6479–6487.
(8) Bensimon, D. *Structure* **1996**, *4*, 885–889.
(9) Hickenboth, C. R.; Moore, J. S.; White, S. R.; Sottos, N. R.; Baudry, J.; Wilson, S. R. *Nature (London)* **2007**, *446*, 423–427.
(10) Encina, M. V.; Lissi, E.; Sarasua, M.; Gargallo, L.; Radic, D. *J. Polym. Sci., Polym. Lett. Ed.* **1980**, *18*, 757–760.
(11) Berkowski, K. L.; Potisek, S. L.; Hickenboth, C. R.; Moore, J. S. *Macromolecules* **2005**, *38*, 8975–8978.
(12) Potisek, S. L.; Davis, D. A.; Sottos, N. R.; White, S. R.; Moore, J. S. *J. Am. Chem. Soc.* **2007**, *129*, 13808–13809.
(13) Karthikeyan, S.; Stephanie, L. P.; Potisek, S. L.; Piermattei, A.; Sijbesma, R. P. *J. Am. Chem. Soc.* **2008**, *130*, 14968–14969.
(14) Matyjaszewski, K.; Xia, J. *Chem. Rev.* **2001**, *101*, 2921–2990.
(15) Pakula, T.; Zhang, Y.; Matyjaszewski, K.; Lee, H.-i.; Boerner, H.; Qin, S.; Berry, G. C. *Polymer* **2006**, *47*, 7198–7206.
(16) Beyer, M. K. *J. Chem. Phys.* **2000**, *112*, 7307–7312.
(17) Skinner, H. A. *Trans. Faraday Soc.* **1945**, *41*, 645–662.

MA8026996